Development of a remote refrigerant leakage detection system for chillers and VRFs

Shunsuke KIMURA [a], *Michio MORIWAKI* [b], *Manabu YOSHIMI* [c], *Shohei YAMADA* [d], *Takeshi HIKAWA* [e], *Shinichi KASAHARA* [f]

[a-f] Technology and Innovation Centre, Daikin Industries, Ltd., Nishi-Hitotsuya, Settsu, Osaka, 566-8585, Japan

[a] shunsuke.kimura@daikin.co.jp, [b] michio.moriwaki@daikin.co.jp, [c] manabu.yoshimi@daikin.co.jp

[d] shouhei.yamada@daikin.co.jp, [e] takeshi.hikawa@daikin.co.jp, [f] shinichi.kasahara@daikin.co.jp

Abstract. In Europe and Japan, owners of large refrigeration and air-conditioning equipment, such as chillers and VRFs, are required by law to carry out regular inspections for refrigerant leaks. There are two methods of regular inspection: the direct method, which uses visual inspection and leak detectors equipped with gas sensors; and the indirect method, which uses equipment operating data to estimate leaks. However, large equipment requires many inspection points and direct inspection is time-consuming and labor-intensive, placing a heavy burden on both the equipment owner and the inspector. On the other hand, the European F-gas regulation provides an incentive to halve the number of inspections if a permanent leakage detection system is installed, and similar incentives are being considered for other countries regulations. The authors developed a highly accurate refrigerant leakage detection system using machine learning techniques that can be used to meet incentive requirements. The details of the technology and the accuracy of the detection system tested on chillers and VRFs are discussed in this paper.

Keywords. refrigerant leakage detection, chiller, VRF, machine learning
DOI: https://doi.org/10.34641/clima.2022.373

1. Introduction

The F-Gas Regulation, which came into force in Europe in 2006, requires refrigeration and air-conditioning equipment with more than 3 kg of refrigerant to be tested for refrigerant leaks on a regular basis. However, it allows that the frequency of inspections to be halved if the equipment is provided with a leakage detection system. This led to a flurry of development of leakage detection systems.

A leakage detection system using remote monitoring data for VRF was also developed by one of the present authors and his colleagues [1]. However, the demand for leakage detection systems didn't grow because there were no specific penalties for non-compliance with regular inspection requirements.

The revision of the F-gas regulation in 2015, which has led to the implementation of penalties in many countries, has once again energised the development of leakage detection systems. In recent years, the development of big data analysis technology has led to numerous proposals of machine learning based refrigerant leakage detection systems.

According to Hosseini *et. al.* [2], 82 papers have been published worldwide on machine learning based air conditioner fault detection systems between 2016 and 2020, 10 of which are on leakage detection. Out of these 10 papers on leakage detection, 6 papers are on VRF. In Japan, Wakui *et. al.* [3] reported on the simulation of a leakage detection system for VRFs using machine learning.

However, most of these papers are validated using simulations or experimental data obtained in laboratories, and only few of them are validated using actual on-site operating data. Therefore, a leakage detection system for VRF equipment during cooling operation that uses machine learning operated on a remote monitoring system was developed, and its detection accuracy was validated using a large amount of on-site data [4-5]. Also, a leakage detection system for chillers was developed applying this technology [6], which has been launched in Europe. Leakage detection function in heating operation for VRFs has also been developed and validated using on-site data. In this paper, the leakage detection system for chillers and for cooling and heating of VRFs are discussed.

2. Methodology

2.1 Overview of the detection sysytem

The leakage detection system estimates the refrigerant charge amount from the operating data acquired from chiller and VRF equipment, and

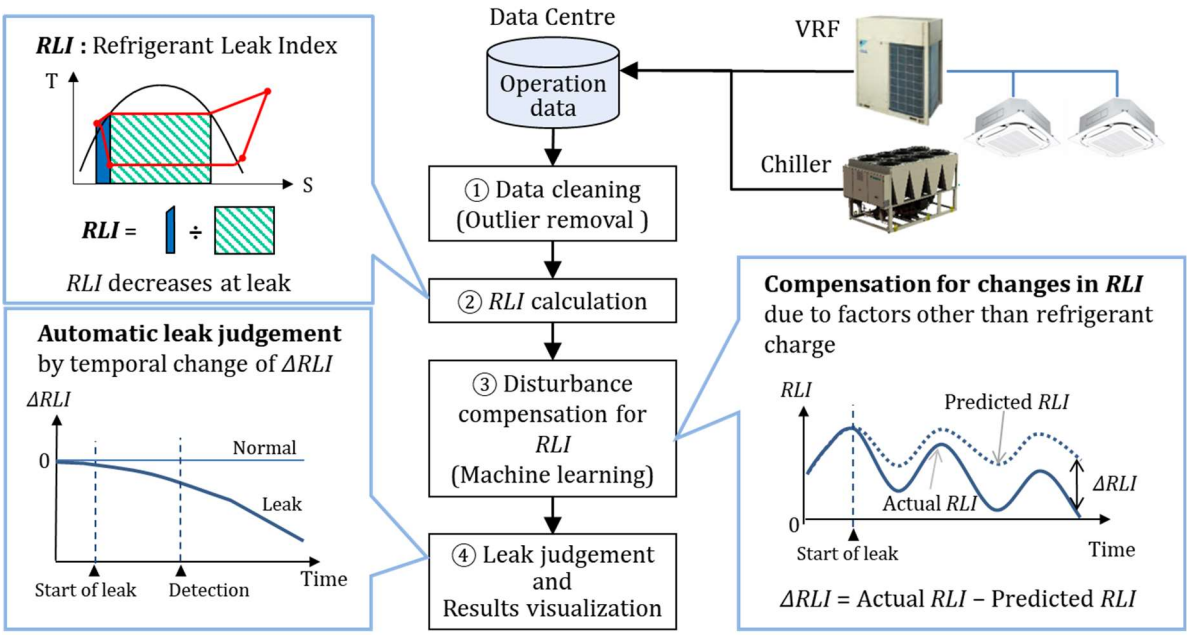

Fig. 1 – Overview of the leakage detection system

automatically detects leakages. Fig. 1 shows an overview of the developed system.

2.2 Refrigerant leak index (RLI)

The leakage detection system calculates the *RLI* (Refrigerant Leak Index), an index strongly correlated with the refrigerant charge amount, from the operating data and detects leakages based on changes in this value.

The *RLI* used in chiller and VRF cooling operations is a dimensionless value defined as the ratio of the area of the liquid region to the area of the saturated region on the T-S diagram, as shown in Fig. 1. As the refrigerant charge amount decreases due to leaks, the *RLI* also decreases.

During the heating operations of the VRF, the degree of superheat of the compressor discharge temperature (*DSH*) is used instead of the above *RLI*. When the refrigerant amount decreases due to leaks, the discharge temperature rises and so does the *DSH*.

The reason why *RLI* is not used during heating is that VRF operates multiple indoor units as condensers during heating, as shown in Fig. 2. The number and types of connected indoor units vary from one to another, and a machine learning model using the *RLI* obtained for each of these indoor units would make the logic very complicated. As a result, the amount of calculation increases, and implementation becomes difficult. Therefore, this VRF-specific challenge was solved by using *DSH* as an index for heating.

2.3 Disturbance compensation for RLI

The *RLI* changes not only due to the refrigerant amount, but also due to external disturbances such as outside temperature and compressor speed. Therefore, even though there is no refrigerant leak, the *RLI* may drop due to the disturbances and the detection algorithm may misjudge it as a leak.

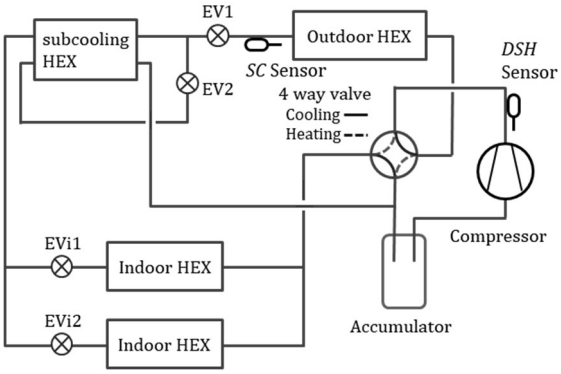

Fig. 2 – Example of VRF piping diagram

To prevent this, the disturbances from *RLI* is removed and the index *ΔRLI*, which represents only the variation of the refrigerant charge amount, is calculated. As shown in Fig. 1, *ΔRLI* is the difference between the actual *RLI* calculated directly from the operating data and the predicted *RLI* under normal conditions. This predicted *RLI* is calculated by a prediction model created using machine learning (ML) from past normal operating data. The disturbances for *DSH*, which is an index for heating, is removed in the same way as above, and *ΔDSH* is calculated as an index of the changes in only the refrigerant charge amount.

To create the *RLI* prediction model for the chillers and the *RLI* and the *DSH* prediction models for the VRFs, ML methods were used according to the characteristics of the respective training data. The specific ML methods and training data acquisition methods for each prediction model are described in the next section.

2.4 How to obtain training data for VRFs and create prediction models

Since VRFs have enough operating data stored in the data centre, it is possible to create an *RLI* prediction model for normal conditions using these as training data. However, the stored data contain both normal data and anomalous data. Normal data means that all functions are normal, and the refrigerant charge amount is appropriate. Anomalous data may be due to malfunctioning components or sensors, or insufficient or excessive refrigerant charge amount.

Therefore, in the process of data cleaning, only normal data were extracted from the stored data as training data for the creation of *RLI* prediction models. The extraction was carried out in the following two stages.

First, the data of equipment without failure records and equipment with completed failure repairs were extracted.

Next, the mean value of *RLI*, an index of refrigerant charge amount, was then calculated for each extracted equipment. The relative frequency distribution of these values is close to the black line of normal distribution curve shown in Fig. 3; the *RLI* value, in other words, the refrigerant charge amount, vary within the range not to be regarded as a failure shown in Fig. 3. This variation is caused by the refrigerant charging process during installation and the refrigerant recovery and recharging process before and after component replacement.

The equipment with a value near the centre of the distribution curve (the red area in the figure) is the equipment charged with the appropriate amount of refrigerant, and its operating data is determined to be available for training.

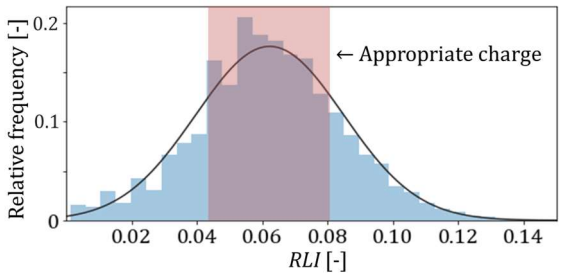

Fig. 3 – Distribution of *RLI*

Using the training data extracted in this way, a prediction model of normal *RLI* was created by LightGBM [7]. The explanatory variables used in the model were outdoor temperature, compressor speed, compressor current, and opening of the expansion valve for subcooling heat exchanger control ("EV2" in Fig. 2). For the training data, data obtained from several different units of the same type were used, instead of using only the data of the target VRF system itself. This is for reducing the operating cost. Therefore, the prediction model will be a common model for that type. The normal *DSH* prediction model for heating was also created in the same way: the explanatory variables in the case of the *DSH* prediction model were outdoor temperature, compressor speed, total capacity of indoor unit in operation and opening of the expansion valve for subcooling heat exchanger control.

The leaks found in the first process and the data during the failure period were labelled according to the failure and used as the anomaly data for the validation of leakage detection accuracy.

2.5 How to obtain training data for chillers and create prediction models

The prediction model for the chiller was created in a different way from that for the VRF. For chillers, the stored data could not be used as training data because there was almost no data of models equipped with a temperature sensor to measure the condenser outlet temperature used for *RLI* calculation. Therefore, a chiller equipped with a sensor for measuring the condenser outlet temperature was installed in a climate chamber, and tests were carried out under various conditions simulating actual operating conditions to obtain training data.

The four test conditions to be varied were outdoor temperature, compressor load ratio, leaving water temperature (*LWT*) and refrigerant charge amount as leak condition. For each condition, the range of variation and the test points within that range were investigated.

If the conditions are set to cover the entire variation range of all parameters uniformly, the number of test man-hours will be huge. Therefore, to create an accurate prediction model while reducing the number of test man-hours, the test conditions were chosen from the frequently occurring operating conditions from the on-site data stored in the data centre.

First, the variation range of the outdoor temperature was set to be between 5 and 35°C, taking into account the European climate. The compressor load ratio was set to vary between 33% and 100%, in line with the specifications of the chiller to be tested. The frequency distributions of the outdoor temperature and the compressor load ratio in the chiller in operation on-site are shown in Fig. 4.

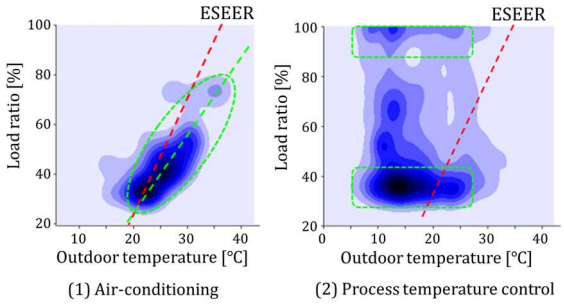

Fig. 4 – Distribution of the combination of outdoor temperature and compressor load ratio

Fig. 4(1) shows the distribution for the air-conditioning application. It shows a similar trend to the ESEER condition which the load ratio is proportional to the outdoor temperature. The centre of the distribution is slightly lower than that of the ESEER condition, which is thought to be due to the larger installed capacity compared to the actual load.

Fig. 4(2) shows the distribution for the process temperature control application in the factory, which is quite different from the distribution for the air-conditioning application: it operates more frequently around the maximum and minimum loads, regardless of the outdoor temperature.

Considering both characteristics, the combinations of test conditions set within the variation range of outdoor temperature and compressor load ratio are shown in Fig. 5. In the 27 conditions set, priority is given to the ESEER condition and the area below the ESEER condition (1), which has a high frequency of occurrence in air-conditioning applications, and to the area (2), which has a high frequency of occurrence in process temperature control applications.

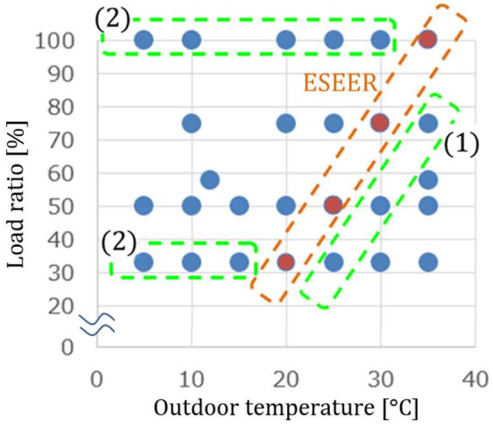

Fig. 5 – Combination of outdoor temperature and compressor load ratio set for the test

The relative frequency distribution of the stored *LWT* data is shown in Fig. 6. It is generally distributed in the range of 2 to 20°C because it is adjusted according to the application and load ratio. The four conditions of 5, 7, 11 and 13°C were chosen to focus on the areas with the highest frequency of occurrence.

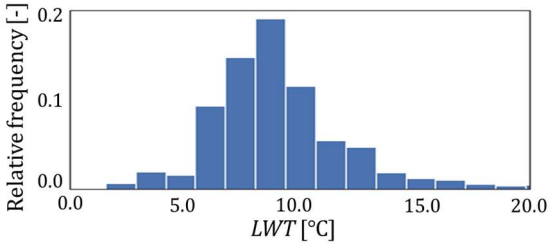

Fig. 6 – Distribution of leaving water temperature

The data obtained from the tests carried out based on the above test conditions were used as training data, and a normal *RLI* prediction model was developed using random forest regression. The six explanatory variables used in the prediction are outdoor temperature, compressor load ratio, *LWT*, main expansion valve opening ("main" in Fig. 7), economizer expansion valve opening ("ec" in Fig. 7) and compressor current.

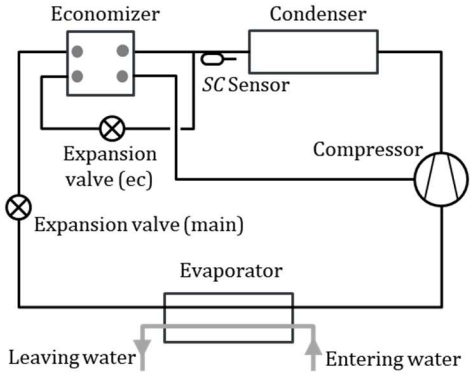

Fig. 7 – Piping diagram of the tested chiller

The training data for the prediction model are randomly selected from 70% of the data with 100% refrigerant charge amount. The remaining data with 100% refrigerant charge amount and the data with 120, 90, 85 and 80% refrigerant charge amount were used as the test data for the validation of leakage detection accuracy.

2.6 Automatic leakage detection logic

The automatic leakage detection logic outputs judgement results of leakage based on the decrease in *ΔRLI*. Fig. 8 shows an overview of the logic for the automatic judgement of refrigerant leakage based on the changes in *ΔRLI* time series data.

The detection logic consists of a moving window with *N* terms, a planar mapping section, an anomaly calculation section and a judgement section. The planar mapping section maps the points whose coordinates are two adjacent points *ΔRLI*(*t*-1) and *ΔRLI*(*t*) onto the plane whose axes are *ΔRLI*(*t*-1) and *ΔRLI*(*t*) at any given time.

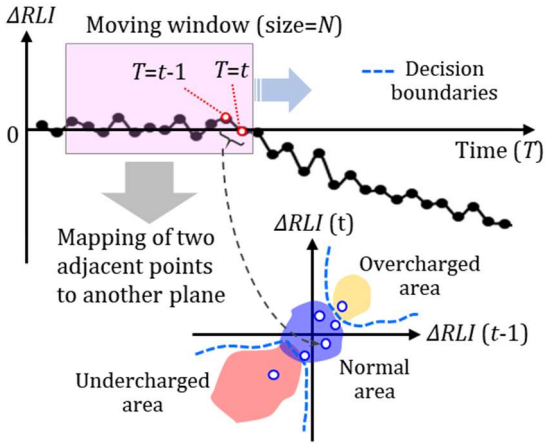

Fig. 8 – Overview of the automatic leakage detection logic

The mapping plane is pre-classified into normal, undercharged, and overcharged areas based on the decision boundaries plotted by machine learning. The undercharged area is in the third quadrant and the overcharged area is in the first quadrant. The anomaly calculation section calculates the anomaly score defined by the following equation (1) when the N-1 points created from the N data in the moving window have been mapped to another plane.

$$Anormaly\ score = \frac{Number\ of\ points\ in\ undercharged\ region}{N-1} \quad (1)$$

The anomaly score is the ratio of the number of N-1 points mapped from the moving window to the number of points mapped in the undercharged area. When this value exceeds a certain threshold, it is judged that there is a leak. If the distribution of points is mapped in the undercharged area from the beginning of operation, it is judged to be undercharged initially. If the distribution of points is mapped in the overcharged area from the beginning of operation, it is judged to be overcharged initially.

In the case of heating, the leakage index is ΔDSH, which increases opposite to ΔRLI during leakage, thus the undercharged area is distributed on the first quadrant.

3. Results and discussion

3.1 VRF data validation results

The responses of *ΔRLI* and *ΔDSH* in VRF equipment were evaluated. Fig. 9 shows the examples during cooling operation; the upper plot for normal equipment and the lower plot for equipment where 15% of the refrigerant charge amount was recovered during operation to simulate a leak.

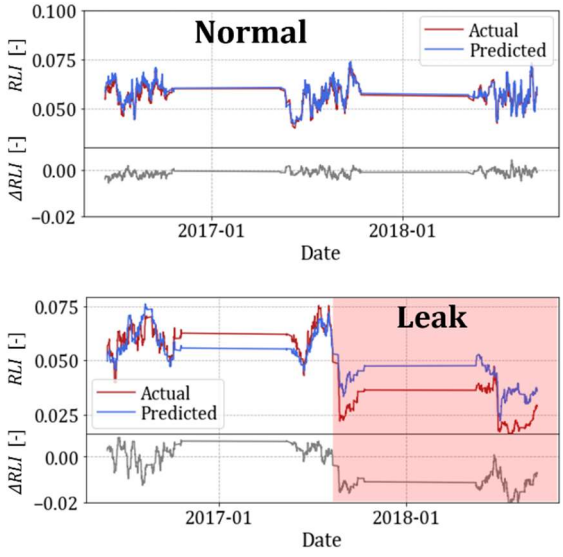

Fig. 9 – *RLI* and *ΔRLI* responses to normal and leak data during cooling operation

Fig. 10 shows the examples during heating operation, the upper plot for normal equipment and the lower plot for leaking equipment. In both Fig. 9 and 10, the red line represents the actual *RLI* and *DSH* calculated directly from the operating data, the blue line represents the *RLI* and *DSH* predicted by the normal prediction model and the grey line at the bottom represents their differences *ΔRLI* and *ΔDSH*, the red areas labelled "Leak" are the period during which the detection logic judged as a leak.

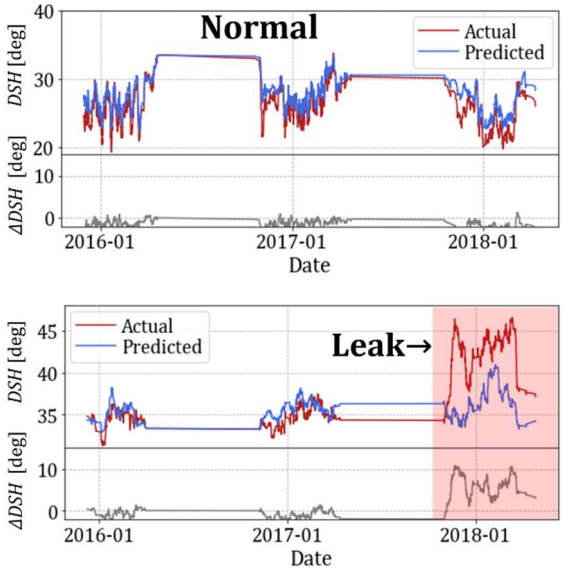

Fig. 10 – *DSH* and *ΔDSH* responses to normal and leak data during heating operation

In normal equipment, the actual values for both cooling and heating are close to the predicted values and the differences, *ΔRLI* and *ΔDSH* are almost 0. On the other hand, during the period when the refrigerant charge decreases in leaking equipment, the actual values for both cooling and heating differ significantly from the predicted values. Thus, the *ΔRLI* and *ΔDSH* values are sufficient for the automatic detection logic to detect the leak correctly.

Next, the leakage detection was carried out for several test data obtained from the stored data and the accuracy of the detection was evaluated from the confusion matrix of the detection results. The confusion matrix is a combination of the correct and incorrect judgment results for the actual equipment state (normal or leaking), and its definition is given in Tab. 1. The judgment performance was evaluated by two indices, accuracy and false discovery rate (*FDR*), as shown below.

$$Accuracy = \frac{TP + TN}{TP + TN + FP + FN} \quad (2)$$

$$False\ discovery\ rate\ (FDR) = \frac{FP}{TP + FP} \quad (3)$$

The accuracy is the ratio of correct predictions among the total number of test cases. The *FDR* is the proportion of normal equipment misclassified as leaks among the equipment classified as leaks.

Tab. 1 - Definition of confusion matrix

		Predicted	
		Normal	Leak
Actual	Normal	TN (True Negative)	FP (False Positive)
	Leak	FN (False Negative)	TP (True Positive)

When assuming the actual operation of a refrigerant leakage detection system, it is important to keep the *FDR* as low as possible. This is because misjudgement of normal equipment as leaking equipment not only increases operating costs due to the unnecessary dispatch of service personnel, but also leads to a loss of user confidence in the detection system. Considering these factors, the target accuracy and *FDR* of the current fault diagnosis by remote monitoring is set to be 80% or higher and 10% or lower, respectively. The detection sensitivity of the automatic leakage detection logic was adjusted to meet the above indices.

Tab. 2 - Confusion matrix of leakage detection evaluation results during cooling

Cooling		**Predicted**	
		Normal	Leak
Actual	Normal	93.7% (119)	6.3% (8)
	Leak	14.9% (7)	85.1% (40)

Tab. 3 - Confusion matrix of leakage detection evaluation results during heating

Heating		**Predicted**	
		Normal	Leak
Actual	Normal	98.8% (82)	1.2% (1)
	Leak	21.5% (6)	78.5% (22)

Tab. 2 and Tab. 3 show the confusion matrices for cooling and heating, respectively, that were calculated after adjusting the detection sensitivity. Each element of the confusion matrix in the table shows the incidence rate of normal and leakage detection against the actual number of normal and leak equipment. The number in () is the number of detections.

Equations (2) and (3) were used to obtain the accuracy and the *FDR* from the confusion matrices for cooling and heating, respectively. The accuracy of 80% or higher and the *FDR* of 10% or lower were achieved in both cooling and heating. The incidence rates in the tables were used for the calculations. The reason is that if there is a large difference between the number of normal equipment and the number of leaking equipment, the judgment result is affected by it. By using the incidence rates, this effect can be eliminated.

Tab. 4 – Accuracy and *FDR* in cooling and heating operation

Operation mode	Cooling	Heating
Accuracy	89.4%	88.7%
FDR	6.9%	1.5%

Finally, the sensitivity of leakage detection was evaluated by obtaining estimates of the leakage amount at the time when the automatic detection logic judged a leak for true positive (TP) equipment. In this paper, the definition of refrigerant leak rate is the ratio of leaked refrigerant amount to the initial charge amount, as commonly used in refrigerant regulations. To estimate the leakage amount at the time of the detection, the conversion coefficient of the changed refrigerant charge amount (% of total refrigerant amount) and *RLI* and *DSH* were determined first. To do this, the data of equipment for which the leakage amount could be identified from the repair records and equipment with intentionally adjusted refrigerant charge amount were used. The leakage amount at the time of the leak detection was calculated by multiplying the change in *RLI* and *DSH* by the conversion coefficient. The relative frequency distribution of the estimated leakage amounts obtained for all the true positive (TP) equipment is shown in Fig. 11. The distribution can be approximated by a normal distribution, and assuming that the mean value of the distribution is defined as the mean detection sensitivity, it was 12.3% for cooling and 13.9% for heating. Assuming a normal distribution as shown by the dotted line in Fig. 11, the worst detection sensitivity is defined as the value of μ+3σ, which is determined from the mean value μ and variance σ, and is estimated to be 19.3% for cooling and 20.3% for heating. Since the current detection logic for VRF has a detection sensitivity of more than 50%, this method improves the detection sensitivity by 30% over the conventional method.

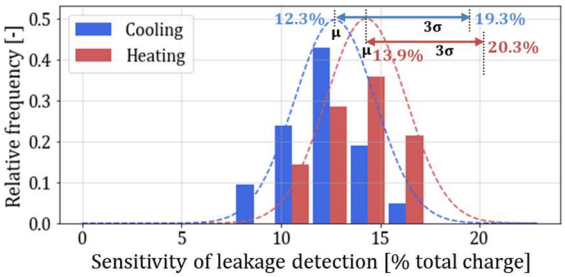

Fig. 11 – Sensitivity of leakage detection in cooling and heating operation

3.2 Chiller data validation results

ΔRLI was calculated using the *RLI* prediction model created with the training normal data obtained in the test chamber, and the responses of *ΔRLI* to normal and leak data were evaluated. Fig.12 shows the examples of measured *RLI,* predicted *RLI* and *ΔRLI*

responses to test data containing normal and leak cases. The test data was taken recovering the refrigerant from 100% to 80% in charge amount. The *ΔRLI*, which was zero at the start of the test, decreases as the refrigerant charge decreases, and the automatic leakage detection logic judges the refrigerant to be leaking around the middle of the transition from 100% to 80%.

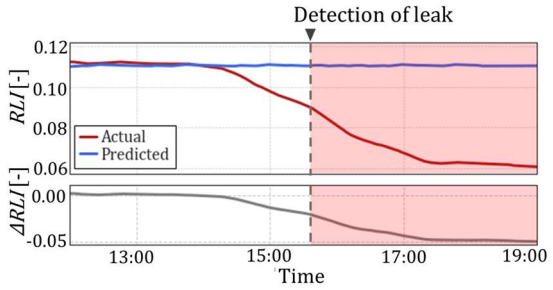

Fig. 12 – Response of *RLI* and *ΔRLI* to changes in refrigerant charge amount

Tab. 5 shows a confusion matrix of the results obtained by performing the same evaluation as above on test data for various operating conditions varying outdoor temperature, compressor load ratio, *LWT* and refrigerant charge amount. The breakdown of test conditions is 56 conditions of normal data with 100% refrigerant charge amount, and 52 conditions of leak data with 85% and 80% refrigerant charge amount. 86.5% of the accuracy and 0% of the *FDR* are calculated by the same method as VRF. However, all normal data are judged as normal, but 14 out of 52 leak data are judged as normal, which means that 26.9% of leak cases are overlooked. This is the reason why the accuracy is lower.

Tab. 5 - Confusion matrix of leakage detection results

		Predicted	
		Normal	Leak
Actual	Normal	56	0
	Leak	14	38

It was found that 12 out of 14 conditions where the leak was misjudged as normal had a compressor load ratio of 58% or less and a *LWT* of 10°C or more. Fig. 13 shows the correlation between refrigerant charge amount and *ΔRLI* when the outdoor temperature and *LWT* are fixed, and the compressor load ratio is varied. As the compressor load ratio decreases, the change in *ΔRLI* for the same change in refrigerant charge amount also decreases, thus reducing the detection sensitivity. Next, to confirm the effect of the *LWT* on the changes in *RLI* and *ΔRLI*, the occurrence rate of subcooling (*SC)* at different *LWT* was checked. Fig. 14 shows the relative frequency distribution of *SC* for 100% and 85% refrigerant charge amount under the conditions of 7°C and 13°C *LWT*. When the *LWT* is 7°C, the *SC* distributions for 100% and 85% of the refrigerant charge amount are separated by a boundary of *SC* =5, whereas when the *LWT* is 13°C, the *SC* distributions for each refrigerant charge overlap, making leakage detection difficult. Furthermore, the accuracy and the false negative rate (*FNR*), where a leak is overlooked and judged normal, were recalculated separately for cases with *LWT* below 10°C and the other above 10°C. As a result, the accuracy was 94.2% below 10°C and the *FNR* was 11.5%. On the contrary, for cases with *LWT* above 10°C, the accuracy was 78.8%, and the *FNR* was 42.3%.

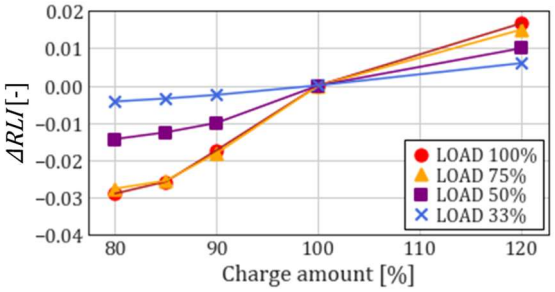

Fig. 13 – Effect of compressor load ratio on the correlation between refrigerant charge amount and *ΔRLI*

Thus, it was found that the chiller operated under the condition of low compressor load ratio and high *LWT* may increase the number of false judgments due to the decrease of leakage detection sensitivity. As a result of analysing the operating data of chillers in operation stored in the data centre, it was found that there are only a few chillers that are always operated at *LWT* of 10°C or higher. It was also found that even if the air-conditioning load decreases during the winter, the chiller operates at a high load and low *LWT* during start-up, so the chiller operates under conditions with high detection sensitivity at least once a day. Therefore, most of the chillers can be operated with this detection logic without any problems.

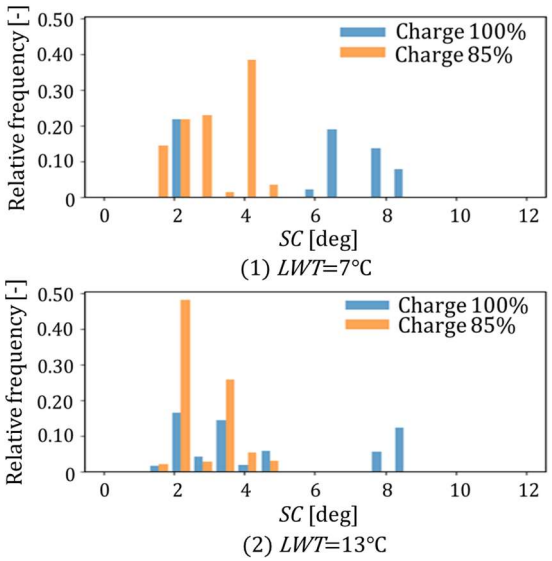

Fig. 14 – Effect of *LWT* on *SC* distribution for different refrigerant charge amount

3.3 Consideration of the limit of detection sensitivity by indirect method

To clarify the theoretical detection sensitivity limit and the feasible detection sensitivity of the indirect method of refrigerant leakage detection, a comparison was made between the simulation study and the results obtained in this study.

Wakui *et. al.* [3] evaluated the refrigerant leakage detection sensitivity of the VRF for several operating conditions using a steady-state refrigeration cycle simulator and a support vector machine classifier. They found that the leak from VRF becomes detectable under some conditions when the leakage amount exceeds 3% of the total charge amount, and when the leakage amount reaches 5%, the leak from VRF becomes detectable with a 100% positive response rate. Therefore, the worst value of the theoretical detection sensitivity characteristics (μ'+3σ') is assumed to be 5%.

On the other hand, as shown in Fig. 11, approximation of the estimated detection sensitivity of VRF during cooling proposed in this study using a normal distribution, the average sensitivity is 12.3% (μ) and the worst detection sensitivity (μ + 3σ) is 19.3%. Fig. 15 shows a schematic diagram comparing these two leakage detection sensitivity distributions.

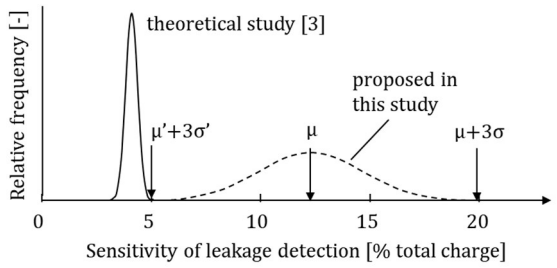

Fig. 15 – Comparison of theoretical and proposed sensitivity of leakage detection in VRF cooling mode

The detection sensitivity distribution by this method has a large variance compared to the theoretical detection sensitivity distribution by the simulation. This is because the machine learning model has not yet properly eliminated the disturbances that affect the detection sensitivity. As a result, when the decision threshold is adjusted so that the accuracy of the leakage detection is 80% or more and the *FDR* is 10% or less as the required level for operation, the detection sensitivity is significantly lower than the theoretical value. However, there is room to improve sensitivity by about 15% by improving the disturbance compensation.

There are two possible reasons for the lower disturbance compensation capability of the machine learning model used in this method compared to the simulation.

The first reason is that the simulation uses steady-state data with fixed compressor inlet pressure and superheat at the evaporator outlet and subcooling HEX outlet for both model training and leakage detection, whereas this method uses non-steady-state daily operating data for both. One possible countermeasure is to periodically set up operating conditions which are fixed to obtain steady-state operating data while VRF is in operation.

The second reason is that the simulation uses a dedicated prediction model for detection, which is created by learning the operating data of the target VRF system itself, while the present method uses a common prediction model as mentioned in chapter 2.4. If a dedicated model is used, sensitivity can be easily improved.

4. Conclusions

An indirect refrigerant leakage detection system based on machine learning was developed and its performance was validated on VRFs and chillers. The detection sensitivity was normally distributed according to the operating conditions and equipment characteristics and was able to detect leaks of 15% of the initial refrigerant charge amount on average and 20% at worst. There is room for improvement in accuracy by modifying the machine learning model and the training data. The next target is to improve the accuracy to detect 10% of leaks in the future.

5. References

[1] Yoshimi M., Yonemori T., Suko K., Yamaguchi T. Proc. The International Symposium on New Refrigerants and Environmental Technology 2010, (2010), pp. 169–172.

[2] Hosseini Gourabpasi A, Nik-Bakht M. Knowledge Discovery by Analyzing the State of the Art of Data-Driven Fault Detection and Diagnostics of Building HVAC. CivilEng. 2021;2(4):986-1008.

[3] Wakui T., Yokoyama R. Proc. of 2018 JSRAE Annual Conference, 2018; C222. (in Japanese)

[4] Yoshimi M., Hikawa T., Kasahara S. Proc. of 2019 JSRAE Annual Conference, 2019; C342. (in Japanese)

[5] Yamada S., Yoshimi M., Hikawa T., Kasahara S. Proc. of 2020 JSRAE Annual Conference, 2020; C323. (in Japanese)

[6] Yamada S., Kojiyama K., Yoshimi M., Kasahara S. Proc. of 2021 JSRAE Annual Conference, 2021; C312. (in Japanese)

[7] https://lightgbm.readthedocs.io/en/latest/

The datasets generated and analysed during the current study are not available due to commercial restrictions, but the authors will make every reasonable effort to publish them in near future.